ADVANCED FUNCTIONAL MATERIALS
www.afm-journal.de

www.MaterialsViews.com

One-Step Formulation of Protein Microparticles with Tailored Properties: Hard Templating at Soft Conditions

Dmitry V. Volodkin, Stephan Schmidt, Paulo Fernandes, Natalia I. Larionova, Gleb B. Sukhorukov, Claus Duschl, Helmuth Möhwald, and Regine von Klitzing*

Formulation of therapeutic proteins into particulate forms is a main strategy for site-specific and prolonged protein delivery as well as for protection against degradation. Precise control over protein particle size, dispersity, purity, as well as mild preparation conditions and minimal processing steps are highly desirable. It is, however, hard to fit all these criteria with conventional preparation techniques. Here a one-step hard-templating synthesis of microparticles composed of functional, non-denatured protein is reported. The method is based on filling porous $CaCO_3$ microtemplates with the protein near to its isoelectric point (pI) followed by pH- or EDTA-mediated dissolution of the tempplates. In principle, a wide variety of proteins can be converted into microparticles using this approach. The main requirement is an overlap of the protein insolubility and a template solubility for a certain parameter (here pH or EDTA). Here the formulation of insulin particles is studied in detail and it is shown that particles consisting of high molecular weight protein (catalase) can also be prepared. In this context, the synthesis of $CaCO_3$ templates with controlled size, the mechanism of the protein microparticle formation and mechanical properties of the microparticles are discussed. For the first time, the fabrication of mesoporous monodispersed $CaCO_3$ microtemplates with identical porocity but tuned diameter from 3 to 20 μm is demonstrated. The protein particle diameter can be adjusted by choosing the appropriate template size that is critical for successful pulmonary delivery of insulin. As a first step towards insulin delivery, the in vitro release of insulin at physiological conditions is studied.

1. Introduction

A wealth of proteins are used as therapeutic agents in clinical practice. This includes vaccines, cytokines, growth factors, blood products, enzymes, etc.[1] Due to the high degradability in the digestive tract and low skin permeability proteins are typically administered by multiple injections, a route often compromised by low patient compliance and low therapeutic performance, e.g., due to localized deposition.[2] Therefore delivery systems with the ability of so-called targeted delivery, sustained release, and protection against degradation are highly appreciated. These requirements can be achieved by protein formulation into particulate systems,[3] e.g., by means of conventional techniques including protein crystallization[4,5] and protein embedding into polymers or lipid matrices.[6–12] For example, release rate of protein microcrystals can be regulated by the crystalline nature and crystal morphology, size and composition.[5,13] It is, however, complicated to control size and dispersity of protein microcrystals to achieve well defined release profile. Therefore, in order to achieve high therapeutic efficacy, particulate drug systems require fine control over particle characteristics, such as size distribution, shape, and morphology. Beyond that, there are a number of requirements regarding the preparation of protein particles: i) mild preparation conditions are necessary to keep protein secondary and tertiary structure intact; ii) purity is an important issue to avoid undesirable side effects, which might arise due to the presence of additives; iii) minimal processing steps are desirable for large-scale production; iv) colloidal stability is required to achieve a long shelf life. It is, however, hard to fulfill all these criteria using conventional techniques, which often lack fine control over particle size distribution or cause protein denaturation due to exposure to high temperature, non-physiological pH, high ionic strength, or hydrophobic interfaces.

For example, spray drying or lyophilization techniques can lead to pure but at the same time polydisperse proteins particles.[7,14] To overcome particle polydispersity template-directed synthesis has been widely applied to assemble well-defined structures with control over internal structure, morphology, composition, etc.[15–23] The most straightforward

Dr. D. V. Volodkin, Dr. S. Schmidt, Dr. C. Duschl
Department Cellular Biotechnology & Biochips
Fraunhofer Institute for Biomedical Engineering IBMT
Am Mühlenberg 13, Golm/Potsdam, 14424, Germany
E-mail: dmitry.volodkin@ibmt.fraunhofer.de
Dr. P. Fernandes, Prof. H. Möhwald
Department of Interfaces
Max-Planck Institute for Colloids and Interfaces
Am Mühlenberg 1, Golm/Potsdam, 14424, Germany
Prof. R. von Klitzing
Stranski-Laboratorium für Physikalische und Theoretische Chemie
Institut für Chemie
Technische Universität Berlin
Strasse des 17. Juni 124, 10623 Berlin, Germany
Prof. G. B. Sukhorukov
Queen Mary Univ London
Sch Engn & Mat Sci, London E1 4NS, England
Prof. N. I. Larionova
Department of Chemistry
Moscow State University
Moscow, 119992, Russia

DOI: 10.1002/adfm.201103007

method towards such assemblies employs inorganic (hard) materials as templates, that are first loaded with the molecules of choice and then removed by applying various stimuli such as selective solvents, pH or temperature. This so-called "hard templating" method is rather ubiquitous, for example it paved the way towards more complex morphologies from self assembling materials such as polymer microcapsules.[19,24] However, such template approaches for the generation of biologically active protein assemblies have been rarely reported, most probably because the conditions for template removal are usually not compatible with protein stability. In this context, Caruso et al. have demonstrated the fabrication of nanoporous protein particles through templating with microporous silica.[21] This method represents a versatile method to fabricate protein particles, which could be only limited by the fact that the template removal requires harsh conditions (2M HF/8M NH_4F) that very likely affect the protein structure due to hydrolysis of disulfide bridges or deamidation. Moreover, in order to stabilize the proteins assembly against dissolution during such conditions, they were stabilized by polyelectrolytes, thus preparation of pure protein particles was not possible.

Templating of protein particles by entrapment into polymer network[25] or by means of inter-protein crosslinking[26] using sacrificial calcium carbonate particles can be done at mild conditions. Porous calcium carbonate microparticles have been introduced in our group as decomposable and bio-compatible templates to fabricate polymeric matrix-type microcapsules by the layer-by-layer polymer adsorption.[25–28] The main advantages of these templates besides ease of preparation include mild decomposition (EDTA or acidic pH) conditions, uniformity and narrow size distribution, highly developed internal architecture (surface area of 8.8 m^2/g). The templates have shown great potential for formulation of polymeric systems with defined shape and internal structure - polymeric microcapsules loaded with material of different sizes and other properties such as small molecules (pharmaceuticals,[29] phospholipids,[30] organic solvents[31]) and large macromolecules (enzymes,[22] DNA,[32]} and polysaccharides[33,34]). Stimuli-sensitive capsules[23,35] were utilized for light-stimulated intracellular delivery.[36] Capsules with more complicated architecture (multi-compartment[37]) have been produced as well.

In a pioneering study we have reported the formulation of spherical insulin microparticles by hard-templating using decomposable porous $CaCO_3$ microparticles.[38] As a model protein we used insulin because of its relevance as a therapeutic protein as well as unresolved delivery issues except for subcutaneous injections.[39] Here we extend this study showing that this approach can be used to fabricate particles using high molecular weight proteins (catalase) and also study how the size of insulin microparticles can be controlled by the choice of the $CaCO_3$ templates. Using optical and electron microscopy we shed light on the composition, morphology and mechanism of the protein particle formation. In addition, mechanical properties of the microparticles are considered as a function of particle size and protein loading. Finally, we discuss pulmonary protein drug delivery using insulin microparticles and, consequently, study in vitro release at physiological conditions.

2. Results and Discussion

2.1. Synthesis of $CaCO_3$ Microtemplates

Vaterite, a polymorph, of $CaCO_3$ is an ideal candidate as a template for protein particles because it is decomposable at relatively mild conditions. Here we have prepared $CaCO_3$ vaterite particles with well defined size using the procedure described in our previous work.[27] The particles were formed at supersaturation by mixing of $CaCl_2$ and Na_2CO_3 under vigorous stirring and initiated by heterogeneous precipitation.[40] This means that mixing of supersaturated salt solutions results in formation of nuclei followed by crystal growth. The higher is the number of initially formed nuclei, the smaller are crystals if the concentration and the amount of salts are kept the same. We have varied two parameters affecting the formation of the nuclei, time and speed of stirring after salt mixing. Increase of both time and speed leads to more pronounced salt intermixing and, as a result, larger number of nuclei and smaller crystals (**Figure 1**). Increase of salt concentration also leads to decrease

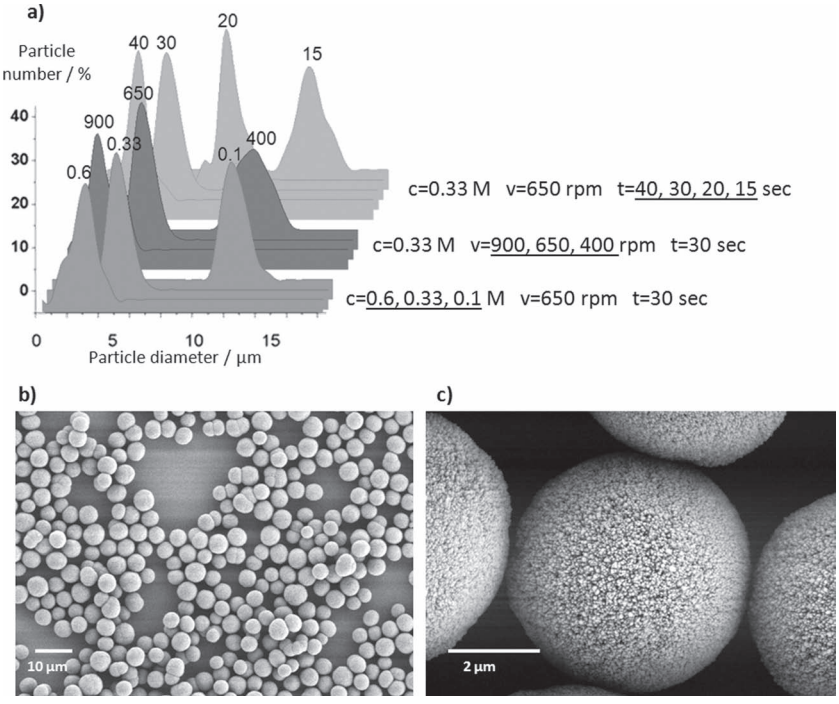

Figure 1. a) $CaCO_3$ particle size distribution as a function of preparation conditions (salt concentration (c), speed (ν) and time (t) of salt stirring). (b,c) - SEM images of the particles with a size of 5.5 µm prepared at $c = 0.33$ M, $\nu = 650$ rpm, $t = 30$ s.

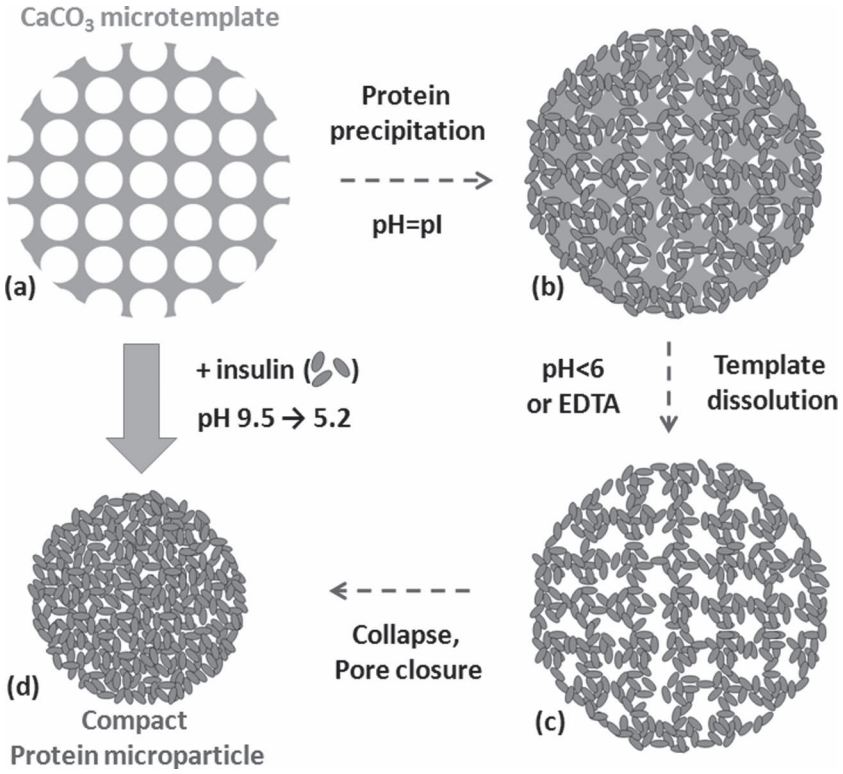

Figure 2. Schematic illustration of the synthesis of protein microparticles. a–b) Loading of porous $CaCO_3$ microtemplates with protein molecules by isoelectric precipitation. b–c) Dissolution of the $CaCO_3$ microtemplate. c–d) Shrinkage of porous protein matrix to a compact microparticle.

in size of the crystals, most probably due to the same reason. In the case of speed variation the stirring time has been kept 30 sec and for time variation the stirring speed has been kept 650 rpm. Particles with average diameter of 3.0 ± 0.9, 5.5 ± 0.6, 15.2 ± 3.8 μm were prepared by variation of the preparation conditions above (Figure 1). Thus, by simply controlling the agitation conditions (stirring time and speed) after salt mixing allows preparing $CaCO_3$ particles with controlled sizes in the range from 3 to 20 μm. The particles have narrow size distribution. Particles with sizes below 3 μm and above 20 μm can also be produced using the same approach but these particles will be more polydisperse.

2.2. Fabrication of Insulin Microparticles

After preparing $CaCO_3$ templates of different sizes, insulin particles were prepared in a one-step procedure as schematically illustrated in **Figure 2**. The procedure consists in titration of insulin solution with HCl in the presence of the template particles (Figure 2a–d). During titration the pH in the solution is decreased from 9.5 to 5.2. Three intermediate steps can be identified during the fabrication process. First, in alkaline medium insulin is soluble and homogeneously distributed in the aqueous phase. Second, at pH values below 7.5 the insulin solubility is dramatically decreased resulting in isoelectric precipitation of the protein[38,41–43] into the pores of the $CaCO_3$ templates (Figure 2a–b). Importantly, the secondary structure of insulin is preserved at isoelectric precipitation.[44] In the presence of $CaCO_3$ insulin precipitates in the pH range 4.5-7.5 as can be observed visually by turbidity increase in solution.[38] Due to a balance of a net charge of aminoacids in the vicinity of the isoelectric point (insulin has an isoelectric point of 5.3[45]) the solubility of the protein is dramatically decreased in water. It can be expected that precipitation of insulin is enhanced at the $CaCO_3$ interface as compared to the bulk solution even at electrostatically repulsive conditions.[46] As a result, insulin enriches within the $CaCO_3$ particles due to their high specific surface area of 8.8 m^2/g.[27] Third, further change of the pH to acidic region (up to pH 5.2) results in dissolution of calcium carbonate, template removal and formation of pure protein particles (Figure 2b–c). In a final step the particles may collapse due to hydrophobic self interaction of the protein resulting in release of water from the pores created after removal of the $CaCO_3$ templates. The formed protein particles are stable in terms of aggregation, a majority of the particles are not aggregated.

Using optical microscopy we study the formation of protein microparticles for each of the intermediate steps, see **Figure 3**. First we discuss particles prepared from templates with an intermediate diameter of 5.5 μm prepared at a protein/$CaCO_3$ weight ratio of 8%. The brightness of the particles in the transmission images (Figure 3) signifies the protein density in the particles. The refractive index of proteins (1.4–1.5)[47,48] is in between the indices for water (1.33) and calcium carbonate (around 1.6).[49] This explains why $CaCO_3$ particles filled with the protein (Figure 3e) are darker than bare templates (Figure 3d), while the particles become brighter (Figure 3f) after removal of the inorganic template. As indicated by the fluorescence channel (Figure 3a) at pH 9.5 insulin was present in the templates at larger concentrations as compared to the bulk solution. This could be caused by formation of a thin layer of insulin on vaterite interfaces. Such protein layers even form on like-charged interfaces[50] as is the case here because the zeta-potentials of insulin[51] and vaterite[25] are both negative. Nevertheless it can be expected that insulin forms a loose layer on the $CaCO_3$ surface that might not be compact due to electrostatic repulsion. The large number of negative charges at pH 9.5 results in intermolecular repulsion and a high solubility of insulin, therefore only small amounts can be loaded into the templates. This agrees well with the results presented in **Figure 4** showing the content of insulin in the supernatant of centrifuged $CaCO_3$ microtemplates at pH 9.5 and 6.2 as a function of the protein/$CaCO_3$ weight ratio. We found that even for the smallest protein/$CaCO_3$ weight ratio of 2% the bulk phase (supernatant) contains the majority of protein at pH 9.5. This means that only a small fraction of protein is contained in the template, whereas in the lower pH range (pH 6.2) the insulin

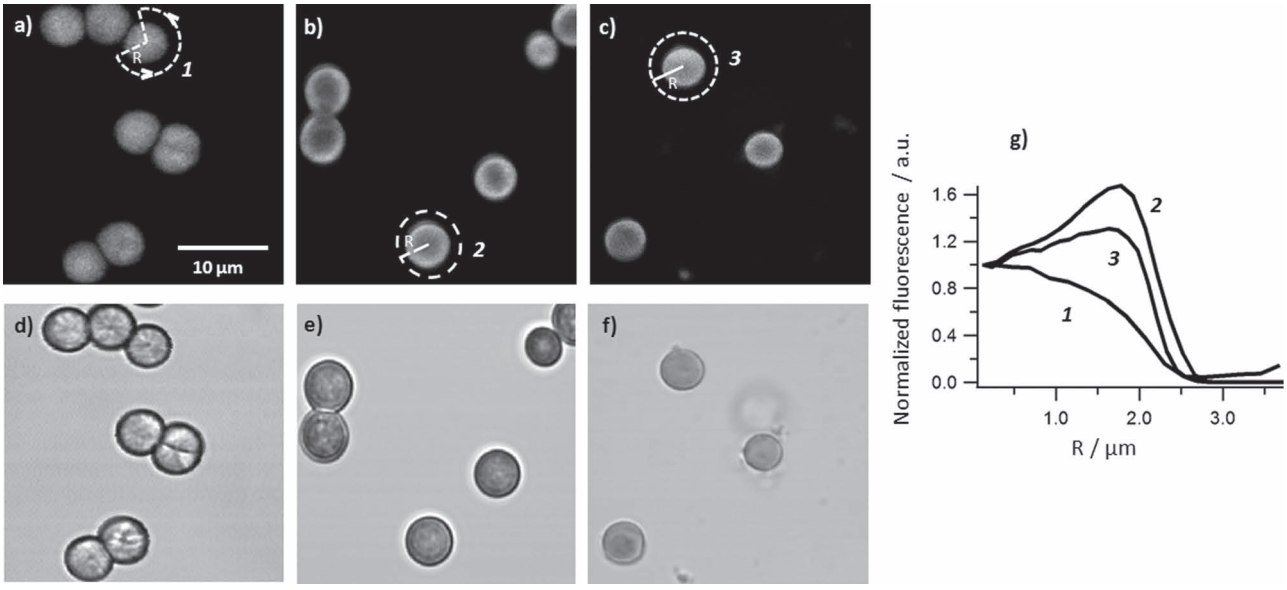

Figure 3. CLSM images of the $CaCO_3$ microtemplates: a,d) in the presence of protein solution at pH 9.5 and b,e) with precipitated protein at pH 6.5. c,f) CLSM images of the protein microparticles with dissolved $CaCO_3$ matrix. a,b,c) Transmission and d.e.f) fluorescence mode with FITC-labeled protein. g) Radial profiles of protein distribution in the particles correspond to the particles chosen in the images (a)–(c). Size of $CaCO_3$ microtemplates 5.5 ± 0.6 µm.

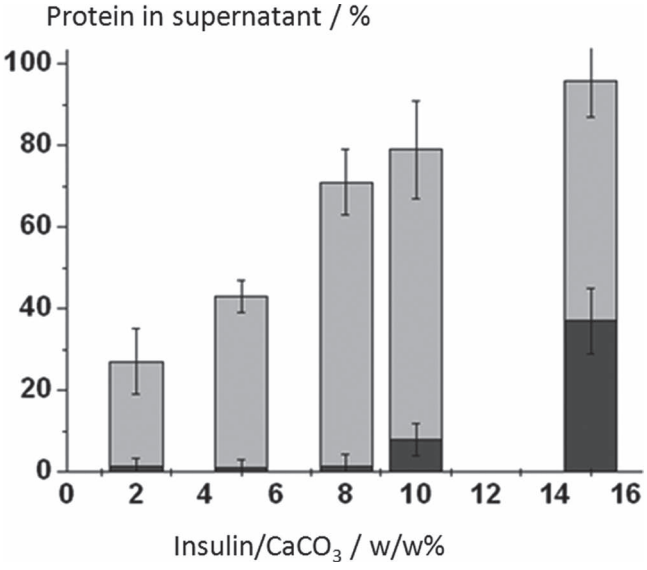

Figure 4. Normalized protein content in the supernatant of the suspension of $CaCO_3$ microtemplates in protein solution at pH values 9.5 (grey) and 6.2 (black) as a function of initial protein/$CaCO_3$ weight ratio.

solubility is decreased and the protein starts to precipitate predominantly into the template particles.

Figure 4 shows that up to a protein/$CaCO_3$ weight ratio of 8% almost all protein was contained in the templates, meaning that precipitation took place in pores of the templates exclusively. At concentrations larger than 8% a significant amount of protein also precipitates outside of the templates as was seen from the increasing insulin absorbance in the supernatant solution (Figure 4, black bars) The protein/$CaCO_3$ weight ratio of 8% therefore represents the threshold upon which the maximum protein loading capacity of the pores is reached, and further protein precipitation proceeds in the bulk (data not shown). According to heterogeneous nucleation theory, the growth of insoluble protein agglomerates in the pores may be initiated by formation of a nucleus at the pore walls. Hence adsorption of protein molecules on the surface of calcium carbonate promotes surface-mediated nucleation followed by precipitate growth. Formation of a nucleus in solution is thermodynamically less favorable and finally protein precipitates exclusively in the pores of the $CaCO_3$ microtemplates.

Moreover, when the pH was decreased to 6.5, insulin was inhomogeneously distributed in the templates, as shown in Figure 3b. This could be caused by a decrease of insulin diffusion through the narrow pores, towards the center of the templates. As a result insulin precipitated preferentially at the rim of the templates. Also after template removal this gradient in protein density is preserved within the pure protein particles (Figure 3c). Radial profiles of protein distribution for $CaCO_3$ microtemplates filled with insulin and insulin microparticles were taken for particles presented in Figure 3. Furthermore, we also observed shrinkage of the protein particles after core removal indicating expulsion of water due to hydrophobic interaction within the particle. Note, that fluorescence images were taken at different pH values that affects the emission efficiency of the fluorescence marker, thus the fluorescence signal cannot be used for comparison of the protein content in the particles.

Besides preparing pure insulin particles via pH-variation as described above, we have also prepared protein particles consisting of catalase using the same method (Supporting Information, Figure S3). This protein has pI in the acidic pH range as insulin has but its larger molecular weight is 50-times larger as compared to insulin. This shows that also very large

Table 1. Sizes of the prepared $CaCO_3$ microtemplates and the respective protein microparticles. The ratio between both quantities is the shrinkage coefficient. The protein density was estimated by taking into account the total amount of particles and insulin as well as the shrinkage coefficient. The aerodynamic diameter was calculated by eq 1.

$CaCO_3$ particles		Protein particles				
diameter, [μm]	pore size, [nm]	Diameter (CLSM), [μm]	Diameter (SEM), [μm]	shrinkage coefficient, [units]	Protein density, [g/cm^3]	Aerodynamic diameter, [μm]
3.0 ± 0.9	28 ± 4	2.2 ± 0.4	2.0 ± 0.8	1.36	0.34 ± 0.09	1.3 ± 0.2
5.5 ± 0.6	25 ± 3	3.5 ± 0.4	3.9 ± 0.9	1.34	0.33 ± 0.07	2.0 ± 0.2
15.2 ± 3.8	26 ± 4	10.5 ± 3.8	9.7 ± 2.9	1.45	0.36 ± 0.10	6.3 ± 2.3

species can be transferred into particulate form by variation of the pH. Retention of activity of encapsulated and released from the particles proteins and enzymes such as catalase is of interest for biological and catalytic applications and will be considered in our future research. Additionally we also showed that insulin particles could be prepared by titration with EDTA instead of titration using HCl. Using this method we dissolved the templates at higher pH (6.5) when $CaCO_3$ is stable and obtained insulin particles of similar morphology (Supporting Information, Figure S2). This shows that the method also works at higher pH which would allow the preparation of a wide variety of protein particles with pIs in the neutral pH range or even in alkaline area. The only prerequisite is that the protein solubility is low enough at the pI such that it precipitates isoelectrically in the $CaCO_3$ templates.

2.3. Control Over Protein Particle Size

Next, we studied protein particles prepared from $CaCO_3$ microtemplates with a different diameter. **Table 1** shows the main characteristics of the templates and their corresponding protein particles. Microtemplates with different diameters of 3.0, 5.5, 15.2 μm were prepared by variation of the stirring time as explained above. **Figure 5** presents typical SEM images of microparticles prepared from a mixture of the microtemplates. All particles were compact particles with diameters close to those found by optical microscopy (Table 1). Although the microtemplates have a different diameter, the average pore diameter was constant and below 30 nm (Table 1) because particles were growing at the same salt concentration, difference in growth conditions was just a number of previously formed nuclei, which determines a final size of the particles after growth. The protein density of insulin microparticles with different sizes was the same, around 0.35 g/cm^3 (Table 1) as a result of similar porocity of the templates. In addition, all protein particles prepared with these microtemplates significantly shrank after template removal with a similar shrinkage coefficient (ratio of the particle diameter to $CaCO_3$ core diameter) of about 1.4 (Table 1). This indicates that the density of the protein is similar regardless of their size. More detailed study on the shrinkage has been recently reported.[38]

The protein loading in the templates is not only limited by the template pore size but also by the time the protein is allowed to diffuse into the templates. Protein molecules did not completely fill the pores if the diffusion time was to short (Supporting information, Figure S1). Interestingly, we observed reduced shrinkage of protein particles prepared from the incompletely filled templates. Here the protein particles posses a pronounced core-shell morphology that possibly shows reduced hydrophobic interactions at the center. Radial profiles provide information about prtein distribution in the particles (Supporting information Figure S1).

After analyzing the particle characteristic via optical microscopy we set out to study the morphology of the particles as the template dissolves. A mixture of $CaCO_3$ microtemplates with various diameters (see above) has been used to prepare protein microparticles. We deliberately stopped the template dissolution when the smaller templates (3.0 and 5.5 μm) were completely dissolved whereas the largest templates (15.2 μm) were only partially dissolved. **Figure 6** shows CLSM and TEM images of $CaCO_3$ microtemplates filled with insulin and particles after template removal or during this process. One can see remainders of the template depicted with an arrow surrounded by a protein shell (Figure 6a,b). The CLSM intensity profile of this particle shows higher fluorescence from the edges of the particle than from the centre due to shrinkage of the protein matrix on the edges (template is dissolved) leading to increase of the protein density. TEM microtome images of particles with partly dissolved $CaCO_3$ microtemplate reveal clearly a corona from the protein, which is located on the rest of the inorganic template (Figure 6d). This confirms that, $CaCO_3$ decomposition starts from the particle edges and continues towards the center of the spherical microtemplate. After complete template removal the protein particle has homogeneous distribution of the protein inside as confirmed by TEM.[38] As can be seen, the non-dissolved $CaCO_3$ template is completely black (Figure 6c). The protein corona is composed of a dense protein matrix; there is no inhomogeneity on the scale of tens of nanometers which would correspond to an average diameter of the pores in the $CaCO_3$ microtemplate (Figure 6d, inset). This indicates that shrinkage of the protein matrix (Figure 2c–d) takes place simultaneously with dissolution of the inorganic template. In case the dissolution is almost complete the amount of $CaCO_3$ detected in the particles is below 2% as found by EDX analysis, This amount could

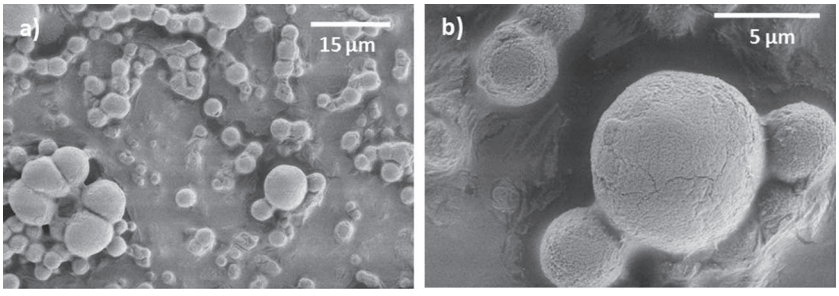

Figure 5. SEM images of the protein microparticles fabricated using a mixture of $CaCO_3$ microtemplates (3.0, 5.5, and 15.2 μm in diameter). (b) is a magnified part of the image (a).

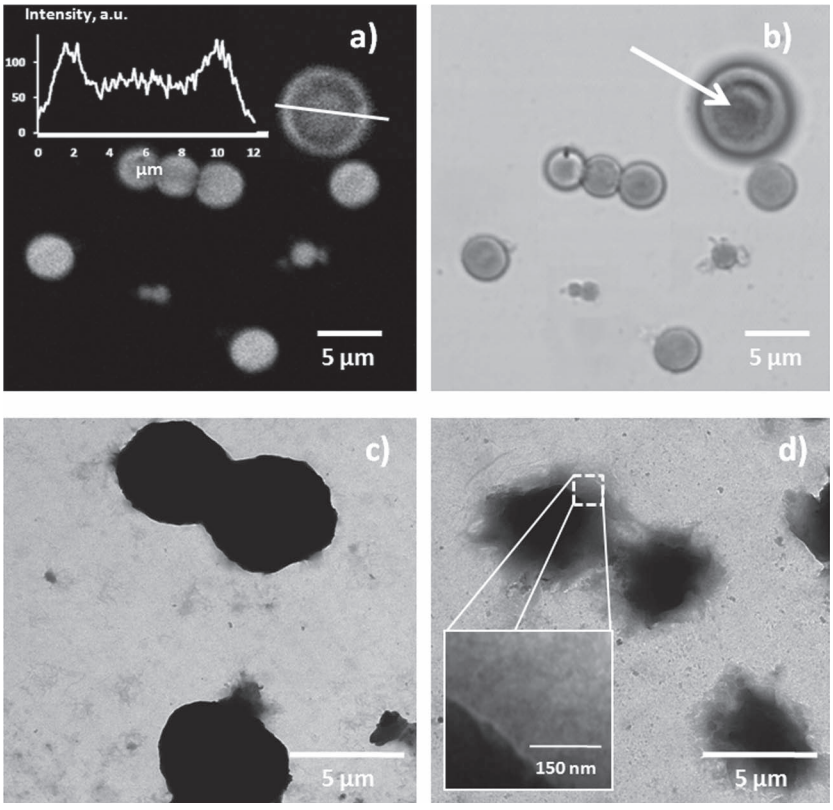

Figure 6. a–b) CLSM fluorescence and transmission images of the protein microparticles fabricated using a mixture of $CaCO_3$ microtemplates with diameters of 3.0, 5.5, and 15.2 µm. c–d) TEM images of the $CaCO_3$ microtemplates (diameter 5.5 µm) filled with precipitated protein before (c) and during (d) dissolution of the template. The inset of the image (d) shows a magnified part of this image.

correspond to Ca^{2+} associated to insulin. A matrix of interpolyelectrolyte complex also has residuals of $CaCO_3$.[25]

2.4. In Vitro Release Study

Release due to dissolution of particulate drug systems can be regulated e.g. by the morphology, size and composition.[5,13] Using the templating approach one can in principle control the release kinetics by adjusting the size of the protein particles. To analyze the range of release kinetics that can be achieved with this system we study the dissolution of the particles at physiological pH and ionic strength. **Figure 7** shows release profiles of insulin from microparticles having an average diameter of 2.2, 3.5, and 10.5 µm, respectively (Table 1). The initial release rate (burst) increases with a decrease of the microparticle diameter which can be explained by a larger surface area of smaller particles. All particles exhibit a burst-like release profile with significant dissolution of 20–40% of the protein within first few minutes followed by a sustained release of minor amounts of insulin in the time scale of hours. This burst-like release profile could be beneficial for protein delivery when a fast decrease of the glucose level for a short time is required. Release of protein molecules from crystals is controlled by the rate of dissociation of protein molecules from the crystal lattice and dependent on a cohesive energy between the molecules as well as on the morphology and composition of the crystal. For the protein microparticles the release profile depends just on the diameter of the particles because the composition and the protein density do not depend on the microparticle size. The release profile can be tuned by the size of the $CaCO_3$ microtemplates giving an option to control the pharmacokinetics. In vivo studies on biological activity of the microparticles will be addressed in our future research.

2.5. Mechanical Properties of the Protein Microparticles

Especially for possible biomedical applications it is important to understand mechanical properties of the prepared protein particles. For example, the mechanical properties of the particles control their aggregation behavior. Hard particles tend to be more stable, whereas softer particles may coalesce and form aggregates. Besides colloidal stability and shelf life the mechanical properties of drug carriers are critical for their in vivo applicability as they may have to sustain shear forces during delivery. Drug carries also need to be mechanically stable to reach the targeted tissue or to penetrate physiological barriers such as kidney, mucus- or epithelium membranes. In the following we discuss the mechanical properties of the particles as a function of their size via AFM colloidal probe measurements. The particles were prepared with the same template but at different insulin/

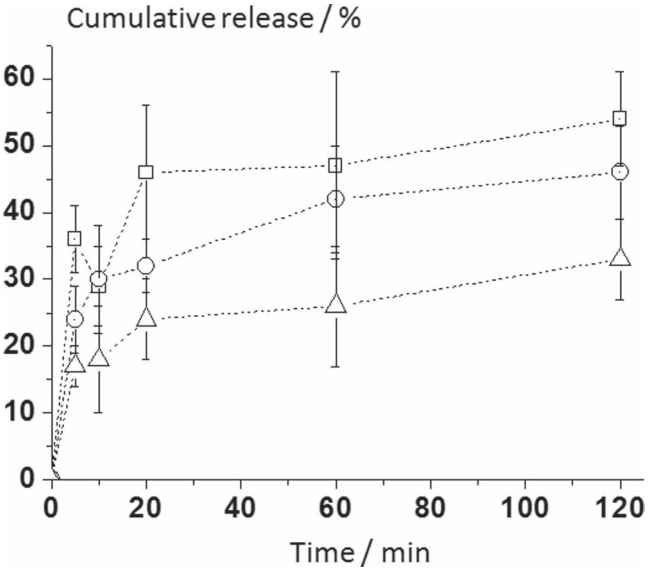

Figure 7. Cumulative protein release profile from the microparticles with diameters 2.2 µm (squares), 3.5 µm (circles), and 10.5 µm (triangles).

Table 2. Sizes and elastic moduli of particles prepared with 5.5 m templates for different insulin/template weight ratio.

Ins/CaCO3 w/w [%]	Particle diameter [μm]	Elastic modulus [kPa]
2	2.4 ± 0.5	112 ± 40
5	3.5 ± 0.6	55 ± 26
10	3.9 ± 0.3	96 ± 37

$CaCO_3$ weight ratio: 2%, 5% and 10%. The resulting insulin particle sizes were, respectively, 2.4 ± 0.5, 3.5 ± 0.6 and 3.9 ± 0.3 μm. The particles were then allowed to sediment on a polystyrene Petri dish at pH 5.2 where they firmly adhered due to hydrophobic interaction with the substrate. Next, AFM force-deformation studies were conducted on individual particles, revealing an elastic modulus of about 100 kPa, irrespective of the particle size (**Table 2**). The size invariance is explained by the fact that for increased insulin/$CaCO_3$ ratios the particles shrink less as compared to lower insulin/$CaCO_3$ ratios.[38] As a result the particles attain the same protein density after shrinkage, regardless of the insulin/$CaCO_3$ weight and resulting particle sizes (Table 1).[38] The obtained modulus of 100 kPa in a typical range for swollen hydrogels[52] and several orders of magnitude smaller than for crystalline protein assemblies.[53] Importantly, the modulus of the partilces larger than the modulus of e.g. the lung tissue (5-30 kPa)[54] which implies sufficient stability of these particles for pulmonary delivery. In our future study we intent to investigate an effect of environmental conditions such as pH, ionic strength, temperature on particle mechanical properties because of importance to understand how the particles will respond to such changes in vivo.

3. Outlook: Potential use for Pulmonary Delivery

Insulin has been used in this study as a model protein, however the proposed method can be generalized for other therapeutic proteins. Insulin is one of the most important therapeutic proteins used to regulate the glucose level in the blood of patients suffering from diabetes. Alternative non-invasive administration routes such as nasal, pulmonary, oral, transdermal, ocular delivery have been intensively investigated[55] to overcome the drawbacks of injections (main administration route) - poor patient compliance due to irritation, pain, itching, stinging, etc. Therefore growing attention has been given to pulmonary delivery.[56–59] The respiratory tract has substantial advantages facilitating rapid drug adsorption: large surface area (around 140 m^2) and relatively low metabolic enzyme activity.[55]

The major challenge for development of efficient protein formulations for pulmonary delivery is to produce protein particles with well-controlled properties: size, shape, and density. The appropriate aerodynamic diameter of the particles lies in the range of a few microns, typically 1–5 μm.[55,56] Edwards has shown that the porosity (density) of protein-containing particles plays a significant role in the inhalation.[60] Particles with lower density can be deposited more efficiently in the deep lungs. At the same time, larger particles (up to 20 μm) can avoid phagocytic clearance until they deliver a payload. Thus, larger particles with lower density are preferred. Porous spherical particles with large geometric diameter (d_g) can, however, have a low aerodynamic diameter (d_a) according to the Equation 1:[61]

$$d_a = d_g(\rho/\rho_{water})^{1/2} \quad (1)$$

where ρ is the density of the particle, ρ_{water} is the density of water (1 g/cm^3).

The protein density in the insulin microparticles is around 0.35 g/cm^3 and does not depend on the size of $CaCO_3$ templates (Table 1). The aerodynamic diameter of the microparticles is thus approximately half of the geometric diameter and is in the range of 1–6 μm (eg 1). The aerodynamic diameter of the microparticles lies within a respirable range for inhalation.[55,56] Hence, these microparticles are potential candidates for protein pulmonary delivery. The monodispersity of the protein microparticles and good aerodynamic characteristics due to low protein density are the key factors to achieve a high systematic bioavailability. Additives in the formulation are critical for pulmonary delivery due to poor enzymatic activity in the lung. Potential complications due to additives in the microparticles can be avoided because the microparticles are composed of pure protein.

Summarizing, the protein particle synthesis by one trigger (pH) can be generalized and used for a variety of therapeutic proteins since many of them have pI within the range 4–7 as insulin has. Examples of the therapeutic proteins include interferon alfa-n3 (trademark ALFERON, pI 5.99), Human Serum Albumin (pI 5.67), growth hormone Pegvisomant (pI 5.27), Alpha-1-proteinase inhibitor (pI 5.37).[1] Furthermore, the dissolution of the $CaCO_3$ templates not only by low pH but also using EDTA can extend the number of suitable pharmaceuticals, e.g. proteins having higher pI values.

4. Conclusions

Monodisperse microparticles from pure protein (insulin or catalase) can be prepared at gentle conditions by hard-templating on decomposable $CaCO_3$ microtemplates via isoelectric precipitation followed by pH- or EDTA-mediated template removal. The diameter of the microparticles can be adjusted by using the appropriate template size. The revealed mechanism of template removal involves shrinkage of the protein matrix from porous to compact due to expulsion of water molecules that is driven by hydrophobic inter-protein interactions. This process can be easily visualized by optical microscopy. The initial dissolution rate of microparticulate protein depends on the microparticle size and increases for smaller particles, most probably as a result of larger surface area, thus allowing modulation of the *in vivo* release kinetics. Because of a short burst-like release profile the microparticles are potentially effective to achieve short-acting therapy, which may close the gap to longer acting formulations involving protein crystals. The microparticles are potential candidates for pulmonary delivery due to appropriate aerodynamic diameter and low protein density. The prerequisites for the approach are i) overlap of the solid template stability and protein insolubility, ii) remaining protein insolubility upon template decomposition. Since the $CaCO_3$ templates can be removed by pH decrease in acidic medium and by EDTA at higher pH values, the approach can be generalized for any

molecule able to precipitate where $CaCO_3$ vaterite templates are stable. Therefore, the approach is applicable for a wide range of proteins covering most pharmaceutically active proteins and peptides if using different ways to precipitate the protein molecules. Crosslinking, salting out, precipitation with organic solvents could be potentially used to achieve this goal.

5. Experimental Section

Particle Preparation: FITC-labeled (I2383) and unlabelled insulin (I5500) from bovine pancreas with content of Zn 0.5% were purchased from Sigma-Aldrich (Germany). The labeled insulin was prepared from unlabelled one with labeling ratio of around one FITC molecule per one insulin molecule. Calcium chloride dihydrate ($CaCl_2{\cdot}2H_2O$, Ultra, Sigma, USA) and Na_2CO_3 (pro analysis, Merck, Germany). The water used in all experiments was prepared in a three stage Millipore Milli-Q Plus 185 purification system and had a resistivity higher than 18.2 MΩ cm. $CaCO_3$ microtemplates were synthesized according to a protocol described in[27] at varied conditions, i.e. concentration of salts, stirring speed and time. Briefly, the crystallization process was initiated by rapid mixing of equal volumes (7.5 ml) of $CaCl_2$ and Na_2CO_3 solutions (with equal salt concentration) in glass of zilindrical shape with 4.8 cm in diameter and 8 cm in height. The mixture was intensively agitated on a magnetic stirrer during certain time (triangular magnetic bar, length 4 cm, side dimension 1.4 cm). The amorphous precipitate formed after mixing has been transformed into microparticles with spherical morphology. Variation of concentration of salts, stirring speed and time has been studied to affect size of the formed particles. One condition has been varied at fixed other two conditions. Salt concentration (equal for both $CaCl_2$ and Na_2CO_3) has been chosen 0.6, 0.33, and 0.1 M; stirring speed and time fixed at 650 rpm and 30 sec, respectively. Stirring speed of 900, 650, and 400 rpm was varied at fixed salt concentration of 0.33 M and stirring time of 30 sec. Stirring time has been chosen 40, 30, 20, and 15 sec at fixed salt concentration of 0.33 M and stirring speed of 650 rpm. The Size of $CaCO_3$ microparticles was calculated using optical transmission images and image processing software for at least 35 particles. Particle size distribution has been presented as a histogram with a bin width 0.5 μm.

For fabrication of insulin microparticles $CaCO_3$ microtemplates were prepared as described above with stirring time for agitation (rotation speed of the stirrer 650 rpm) of supersaturated precursor solutions of $CaCl_2$ and Na_2CO_3 of 45, 30, 10 sec. Concentration of the salts Na_2CO_3 and $CaCl_2$ was the same, 0.33 M. The average particle diameter was found to be 3.0 ± 0.9, 5.5 ± 0.6, 15.2 ± 3.8 μm, respectively. Either a mixture of the microtemplates of various diameters (20% of 3.0 μm, 60% of 5.5 μm and 20% of 15.2 μm particles, w/w%) or microtemplates of a defined diameter were used to prepare the protein microparticles as follows: 10 mg of $CaCO_3$ particles were dispersed in 15 mL of insulin solution with pH adjusted to 9.5. For insulin particles, the stock protein solution contains 10% (w/w) of insulin-FITC compared to unlabelled protein. The suspension was slowly (90 min) titrated with 0.1M HCl till pH 5.2 followed by 1 day dialysis (Float-A-Lyser G2 dialysis tubes, cut-off 0.5–1 kDa, Spectra/Por, USA) against 2L of water with pH adjusted to 5.2. As an alternative to the titration with HCl the template suspension was also titrated with 0.05 M EDTA adjusted to pH 6.5. Here the titration was conducted until the pH of the suspension was 6.5 as well. The microparticles were stored at 4°C as a suspension or lyophilized. All experiments were carried out at room temperature. To study the saturation of the $CaCO_3$ microtemplates with the protein, the initial protein/$CaCO_3$ mass ratio was varied from 2 to 15%. The protein density has been calculated taking into account the average size of the protein microparticles, size and mass of the $CaCO_3$ particles[27] as well the amount of the loaded protein, considering that the number of initial $CaCO_3$ templates is equaled to the number of protein microparticles.

In Vitro Release: For release experiments, a freshly prepared suspension of the protein microparticles fabricated using $CaCO_3$ microtemplates of defined diameters (3.0, 5.5, and 15.2 μm) was replaced by PBS buffer to give a final protein concentration of 0.08 mg/mL. An aliquot of the suspension was taken in defined time intervals and centrifuged (2 min, 5000 g). Fluorescence of the supernatant was analysed using a calibration curve for insulin in PBS buffer. 100% of the release protein corresponds to total dissolution of the microparticles.

Optical Microscopy: CLSM microscopy images were taken with a Leica confocal scanning system mounted on a Leica Aristoplan apparatus and quipped with a 100x oil immersion objective (numerical aperture 1.4). Images of insulin microparticles taken in transmission mode were collected at the same conditions in terms of light illumination.

TEM: Transmission electron microscopy (TEM) images were recorded using the instrument Omega 912 (Carl Zeiss, Oberkochen, Germany) at an acceleration voltage of 120 kV. To identify the internal structure, the microparticles were cut with a microtome. Firstly, the particles were embedded in a polymer matrix using Spurr's embedding medium. After polymerization the resin was dried and thin slices were produced using an ultra microtome.

Nitrogen Adsorption: The pore size distributions of $CaCO_3$ microtemplates were determined following the Brunauer-Emmett-Teller method of nitrogen adsorption/desorption at 77 K, the data being collected with a Micromeritics TriStar system.

SEM/EDX: For scanning electron microscopy (SEM) analysis, samples were prepared by applying a drop of the particle suspension to a glass slide and then drying overnight. The samples were sputtered with gold and measurements were conducted using a Gemini Leo 1550 instrument at an operation voltage of 3 keV. Energy dispersive X-ray (EDX) analysis was performed on the samples prepared similar to the SEM samples. The analysis was done with a Link EDX system from Oxford Instruments with an optimal resolution of 133 eV.

AFM Force Measurements: Atomic force microscopy (AFM) was performed on a "Nanowizard I" AFM (JPK Instruments AG, Berlin, Germany) in an open polystyrene Petri dish containing 20 mM acetate buffer at pH 5.2. As force probes we used silica particles with a diameter of 18 μm (Microparticles GmbH, Berlin, Germany). Using epoxy glue (UHU GmbH & Co. KG, Germany) the probes were attached to silicon cantilevers (NSC 12 Tipless No Al, Mikromasch, Estonia) with a nominal spring constant of 0.2 N/m. The spring constants of the cantilevers were derived using the thermal noise method before attaching the colloidal probes. After attaching the colloidal probes, the cantilever was treated in air plasma at a pressure of 1mbar for 2 min applying an intensity of 18 W (PDC-32G plasma cleaner, Harrick, USA). Prior to the measurements, the protein particles were allowed to sediment and attach to the Petri dish surface by which they are immobilized. The AFM head is mounted on an optical microscope (IX51, Olympus, Japan). Using FITC fluorescence to image the gels the colloidal probe was positioned at the apex of the protein particles in order to perform the AFM force measurement. The measurement was conducted using an approach speed of 1 μm/sec applying a maximum load of 10 nN. The Youngs modulus of the proteins particles was determined by fitting the experimental force versus deformation curves to the Hertz model.[62]

Supporting Information

Supporting Information is available from the Wiley Online Library or from the author.

Acknowledgements

D.V.V. thanks Alexander von Humboldt Foundation for support (AvH Fellowship and Sofja Kovalevskaja Program). We also thank Rona Pitschke and Heike Runge for SEM and TEM imaging.

Received: December 12, 2011
Published online: February 8, 2012

[1] www.drugbank.ca (accessed January 2012).
[2] J. S. Skyler, *Diabetes Care* **1986**, *9*, 666.
[3] S. X. Yang, W. E. Yuan, T. Jin, *Expert Opin. Drug Delivery* **2009**, *6*, 1123.
[4] S. K. Basu, C. P. Govardhan, C. W. Jung, A. L. Margolin, *Expert Opin. Biol. Ther.* **2004**, *4*, 301.
[5] S. Pechenov, B. Shenoy, M. X. Yang, S. K. Basu, A. L. Margolin, *J. Controlled Release* **2004**, *96*, 149.
[6] W. Wang, *Int. J. Pharm.* **2000**, *203*, 1.
[7] Y. F. Maa, P. A. Nguyen, T. Sweeney, S. J. Shire, C. C. Hsu, *Pharm. Res.* **1999**, *16*, 249.
[8] S. Stolnik, L. Illum, S. S. Davis, *Adv. Drug Delivery Rev.* **1995**, *16*, 195.
[9] M. L. Tan, P. F. M. Choong, C. R. Dass, *Peptides* **2010**, *31*, 184.
[10] D. V. Volodkin, N. G. Balabushevitch, G. B. Sukhorukov, N. I. Larionova, *STP Pharm. Sci.* **2003**, *13*, 163.
[11] D. V. Volodkin, N. G. Balabushevitch, G. B. Sukhorukov, N. I. Larionova, *Biochemistry (Moscow)* **2003**, *68*, 236.
[12] F. Caruso, H. Mohwald, *J. Am. Chem. Soc.* **1999**, *121*, 6039.
[13] D. T. Graham, A. R. Pomeroy, *J. Pharm. Pharmacol.* **1984**, *36*, 427.
[14] R. Vehring, *Pharm. Res.* **2008**, *25*, 999.
[15] Y. N. Xia, B. Gates, Y. D. Yin, Y. Lu, *Adv. Mater.* **2000**, *12*, 693.
[16] X. W. Lou, L. A. Archer, Z. C. Yang, *Adv. Mater.* **2008**, *20*, 3987.
[17] G. Decher, *Science* **1997**, *277*, 1232.
[18] X. S. Zhao, F. B. Su, Q. F. Yan, W. P. Guo, X. Y. Bao, L. Lv, Z. C. Zhou, *J. Mater. Chem.* **2006**, *16*, 637.
[19] F. Caruso, R. A. Caruso, H. Mohwald, *Science* **1998**, *282*, 1111.
[20] Z. F. Dai, A. Heilig, H. Zastrow, E. Donath, H. Mohwald, *Chem. A Eur. J.* **2004**, *10*, 6369.
[21] Y. J. Wang, F. Caruso, *Adv. Mater.* **2006**, *18*, 795.
[22] J. Li, Z. Y. Jiang, H. Wu, L. Zhang, L. H. Long, Y. J. Jiang, *Soft Matter* **2010**, *6*, 542.
[23] C. Dejugnat, G. B. Sukhorukov, *Langmuir* **2004**, *20*, 7265.
[24] E. Donath, G. B. Sukhorukov, F. Caruso, S. A. Davis, H. Möhwald, *Angew. Chem. Int. Ed.* **1998**, *37*, 2201.
[25] D. V. Volodkin, N. I. Larionova, G. B. Sukhorukov, *Biomacromolecules* **2004**, *5*, 1962.
[26] W. C. Mak, R. Georgieva, R. Renneberg, H. Baumler, *Adv. Funct. Mater.* **2010**, *20*, 4139.
[27] D. V. Volodkin, A. I. Petrov, M. Prevot, G. B. Sukhorukov, *Langmuir* **2004**, *20*, 3398.
[28] G. B. Sukhorukov, D. V. Volodkin, A. M. Günther, A. I. Petrov, D. B. Shenoy, H. Möhwald, *J. Mater. Chem.* **2004**, *14*, 2073.
[29] C. Wang, C. He, Z. Tong, X. Liu, B. Ren, F. Zeng, *Int. J. Pharm.* **2006**, *308*, 160.
[30] K. Gopal, Z. Lu, M. M. de Villiers, Y. Lvov, *J. Phys. Chem. B* **2006**, *110*, 2471.
[31] C. Deng, W.-F. Dong, T. Adalsteinsson, J. K. Ferri, G. B. Sukhorukov, H. Mohwald, *Soft Matter* **2007**, *3*, 1293.
[32] T. Borodina, E. Markvicheva, S. Kunizhev, H. Möhwald, G. B. Sukhorukov, O. Kreft, *Macromol. Rapid Commun.* **2007**, *28*, 1894.
[33] B. G. De Geest, R. E. Vandenbroucke, A. M. Guenther, G. B. Sukhorukov, W. E. Hennink, N. N. Sanders, J. Demeester, S. C. De Smedt, *Adv. Mater.* **2006**, *18*, 1005.
[34] K. Surendrakumar, G. P. Martyn, E. C. M. Hodgers, M. Jansen, J. A. Blair, *J. Controlled Release* **2003**, *91*, 385.
[35] S. Schmidt, P. A. L. Fernandes, B. G. De Geest, M. Delcea, A. G. Skirtach, H. Mohwald, A. Fery, *Adv. Funct. Mater.* **2011**, *21*, 1411.
[36] S. De Koker, B. G. De Geest, C. Cuvelier, L. Ferdinande, W. Deckers, W. E. Hennink, S. C. De Smedt, N. Mertens, *Adv. Funct. Mater.* **2007**, *17*, 3754.
[37] O. Kreft, M. Prevot, H. Möhwald, Gleb B. Sukhorukov, *Angew. Chem. Int. Ed.* **2007**, *46*, 5605.
[38] D. V. Volodkin, R. von Klitzing, H. Möhwald, *Angew. Chem. Int. Ed.* **2010**, *49*, 9258.
[39] N. A. Peppas, N. J. Kavimandan, *Eur. J. Pharm. Sci.* **2006**, *29*, 183.
[40] L. Brecevic, D. Kralj, *Croat. Chem. Acta* **2007**, *80*, 467.
[41] K. Hallasmoller, K. Petersen, J. Schlichtkrull, *Science* **1952**, *116*, 394.
[42] J. Schlichtkrull, *Acta Chem. Scand.* **1956**, *10*, 1455.
[43] M. L. Brader, M. Sukumar, A. H. Pekar, D. S. McClellan, R. E. Chance, D. B. Flora, A. L. Cox, L. Irwin, S. R. Myers, *Nat. Biotechnol.* **2002**, *20*, 800.
[44] M. M. Bailey, E. M. Gorman, E. J. Munson, C. Berkland, *Langmuir* **2008**, *24*, 13614.
[45] A. Conwayja, L. M. Lewin, *Anal. Biochem.* **1971**, *43*, 394.
[46] S. H. Mollmann, L. Jorgensen, J. T. Bukrinsky, U. Elofsson, W. Norde, S. Frokjaer, *Eur. J. Pharm. Sci.* **2006**, *27*, 194.
[47] J. Vörös, *Biophys. J.* **2004**, *87*, 553.
[48] D. B. Hand, *J. Biol. Chem.* **1934**, *108*, 703.
[49] R. Vogel, M. Persson, C. Feng, S. J. Parkin, T. A. Nieminen, B. Wood, N. R. Heckenberg, H. Rubinsztein-Dunlop, *Langmuir* **2009**, *25*, 11672.
[50] G. Ladam, P. Schaaf, G. Decher, J.-C. Voegel, F. J. G. Cuisinier, *Biomol. Eng.* **2002**, *19*, 273.
[51] A. Taluja, Y. H. Bae, *Pharm. Res.* **2007**, *24*, 1517.
[52] P. A. L. Fernandes, S. Schmidt, M. Zeiser, A. Fery, T. Hellweg, *Soft Matter* **2010**, *6*, 3455.
[53] S. Guo, B. B. Akhremitchev, *Langmuir* **2008**, *24*, 880.
[54] I. Levental, P. C. Georges, P. A. Janmey, *Soft Matter* **2007**, *3*, 299.
[55] E.-S. Khafagy, M. Morishita, Y. Onuki, K. Takayama, *Adv. Drug Delivery Rev.* **2007**, *59*, 1521.
[56] J. Patton, *Curr. Med. Res. Opin.* **2006**, *22*, S5.
[57] J. S. Patton, J. Bukar, S. Nagarajan, *Adv. Drug Delivery Rev.* **1999**, *35*, 235.
[58] J. S. Patton, P. R. Byron, *Nat. Rev. Drug Discovery* **2007**, *6*, 67.
[59] C. Klingler, B. W. Müller, H. Steckel, *Int. J. Pharm.* **2009**, *377*, 173.
[60] D. A. Edwards, J. Hanes, G. Caponetti, J. Hrkach, A. BenJebria, M. L. Eskew, J. Mintzes, D. Deaver, N. Lotan, R. Langer, *Science* **1997**, *276*, 1868.
[61] L. J. Shi, C. J. Plumley, C. Berkland, *Langmuir* **2007**, *23*, 10897.
[62] H. Hertz, *J. Reine Angew. Math. (Crelles Journal)* **1882**, *1882*, 15.